Bioresource Technology Reports 12 (2020) 100555

Contents lists available at ScienceDirect

Bioresource Technology Reports

journal homepage: www.journals.elsevier.com/bioresource-technology-reports

Characterization and bioremediation potential of byproducts from hydrothermal liquefaction of food wastes

Michael James Stablein[a], Aersi Aierzhati[a], Jamison Watson[a], Buchun Si[b], Yuanhui Zhang[a,*]

[a] Department of Agricultural and Biological Engineering, University of Illinois at Urbana-Champaign, Urbana, IL 61801, USA
[b] Laboratory of Environment-Enhancing Energy (E2E), Key Laboratory of Agricultural Engineering in Structure and Environment, Ministry of Agriculture, College of Water Resources and Civil Engineering, China Agricultural University, Beijing 100083, China

ARTICLE INFO

Keywords:
Hydrothermal liquefaction
Food waste
Byproduct characterization
Nutrients availability

ABSTRACT

Hydrothermal Liquefaction is a thermochemical process that uses heat and pressure to convert biowastes into renewable biocrude oil, simultaneously generating both a metal and phosphorus rich solid phase and a nutrient rich aqueous phase. Eight types of food waste, all collected from a campus dining hall and grouped into lipid-rich, protein-rich, and carbohydrate-rich feedstocks, were processed with conditions ranging from 280–340 °C and 10–60 min reaction time. The byproducts for the optimized oil yield conditions were analyzed to elucidate mechanisms by which compounds are concentrated in different phases through their characterization. The differences in elemental and biochemical composition among feedstocks demonstrate considerable gaps in understanding the expected characteristics as a result of several reaction parameters and how to best reuse the materials. This work additionally reviews considerations for subsequent anaerobic digestion and algae cultivation with respect to the nutrients and inhibitory contents of the Hydrothermal Liquefaction Aqueous Phase.

1. Introduction

Food Waste is amounting to as much as 40 million tons per year across the US (EPA, 2019). Typically, both food that is unsuitable for human consumption and food that is wasted after eating is deposited in landfills, amounting to as much as $172 billion in wasted food, and this can additionally result in nutrient leaching into water bodies and greenhouse gas emissions, as well as socioeconomic effects (Danthurebandara et al., 2013) when not disposed of properly. Development of new strategies for advanced value recovery and waste to energy systems is paramount in order to effectively manage the large volume and heterogeneity of such agricultural and industrial wastes.

Hydrothermal Liquefaction (HTL) is a thermochemical process that uses high heat and pressure to convert materials wet organic biowastes, such as swine manure, wastewater sludge, algae biomass, plastic, and food waste, etc. (Aierzhati et al., 2019; Vardon et al., 2011; Wang et al., 2014). into renewable biocrude oil that can be upgraded for fuel (Skaggs et al., 2018), simultaneously generating both a metal and phosphorus rich solid phase and a nutrient rich, toxic aqueous phase (Biller et al., 2012; Jena et al., 2011). HTL has been widely studied in batch reactions and small continuous systems for a number of feedstocks and operating conditions (Cao et al., 2017; Gollakota et al., 2018). The biocrude has properties similar to petroleum, making it suitable for upgrade to transportation fuel (Chen et al., 2018). Researchers have been able to optimize these processes to determine the best substrate properties and liquefaction conditions for biocrude production while working on scale up of HTL and its future applications.

While biocrude and reaction mechanisms for has garnered attention for HTL research, there has been less focus on byproduct valorization. It has been widely suggested that the aqueous phase can be used for value recovery through algae cultivation (Biller et al., 2012; Jena et al., 2011) or leveraged for energy production through anaerobic digestion (Tommaso et al., 2015; Zheng et al., 2017; Zhou et al., 2015) because of its dense concentration of nitrogen and phosphorus nutrients and organic compounds (Watson et al., 2019). The inorganic compounds concentrated in the solid phase, on the other hand, have been recognized for use as asphalt binder, an adsorbent, or for metals recovery (Liu et al., 2017), but they can present bottlenecks in HTL scale up processes, as it can clog the reactor system and hinder the commercial application (Elliott et al., 2015). While the literature covers different HTL feedstocks and byproduct generation (Maddi et al., 2017), analysis of nutrient availability and concentration requirements for post-treatments systems is lacking. Novel and impactful studies must identify abundant, high yielding feedstocks, such as food waste (Aierzhati et al., 2019), that will be leveraged in expanded HTL applications for implementation of waste to energy technologies in society.

* Corresponding author at: 1304 W. Pennsylvania Ave, Urbana, IL 61801, USA.
E-mail address: yzhang1@illinois.edu (Y. Zhang).

https://doi.org/10.1016/j.biteb.2020.100555
Received 26 August 2020; Accepted 26 August 2020
Available online 05 September 2020
2589-014X/

Given heterogeneity of food waste, development of best practices for sorting feedstock and resultant HTL byproducts should consider specific augmentation or removal of such lipid, carbohydrate, and protein-rich materials. To assess byproduct value recovery potential based on these feedstock compositions, food waste derived from a campus dining hall and its model compound components were variably processed to quantify and compare valuable nutrient and organics concentrations. The key innovation of this study to determine key micro and macronutrient availability and characteristics of hydrothermal liquefaction aqueous phase (HTL-AP) and solid products for improved reuse in biological systems. Thus, characterization of HTL aqueous phase and solid residue, as well as reaction conditions influencing their production, will allow for assessing new HTL byproduct applications and limitations to simultaneously derive new value and eliminate waste streams for further HTL implementation.

2. Materials and methods

2.1. Feedstock

The HTL reactions performed for this study used a food waste mixture (M) collected from a dining hall at University of Illinois at Urbana Champaign (Champaign, IL). The food waste was collected and homogenized in a blender to reduce the particle size and consistency. The protein, carbohydrate, and lipid contents could vary for different batches of collected sample, thus varies HTL product yield and distribution. It is important to separate the subcomponents of the food waste and their biochemical composition to determine their effect on HTL processes. These subcomponents were categorized into three groups: high lipid content – salad dressing (L1), cream cheese (L2); high protein content – beef (P1), chicken (P2); and high carbohydrate content – hamburger bun (C1), vegetable (C2), and fruit peels (C3). A mixture of tomato, carrot, and broccoli were mixed in a 1:1:1 wt ratio to compose the vegetable feedstock. Orange and banana peels were mixed in a 1:1 wt ratio for the generation of the fruit peel feedstock.

2.2. Feedstock pretreatment and analysis

Feedstock samples were processed gravimetrically for determination of protein, lipid, and carbohydrates (Midwest Laboratories; Omaha, NE). Total carbon/hydrogen/nitrogen were measured using an Exeter Analytical CE-440 Elemental Analyzer. HHV of the feedstocks was determined using a bomb calorimeter (Model 6200, Parr Instruments Co.; Moline, IL). The elemental and bio-chemical composition (lipids, proteins, carbohydrates), moisture and ash content, and higher heating value (HHV) of the raw materials are provided in another paper (Aierzhati et al., 2019). These compositions are within the range of normal compositions for different feedstocks used in previous HTL experiments (Skaggs et al., 2018). Feedstock samples were placed in a refrigerator at 4 °C for storage during preparation for HTL experiments. Deionized water was used to dilute samples as needed to achieve desired moisture content and served as the reaction solvent.

2.3. Hydrothermal liquefaction of food waste

The solids content was adjusted to 20 wt% for all feedstocks, and HTL reactions were individually performed at 280 °C, 300 °C, 320 °C, 340 °C, and 360 °C for between 10 and 60 min in stainless steel cylinder batch reactors. The pressure range for the reactions was between 1.2 MPa to 11.0 MPa. Additional reactions were performed at 380 °C for two of the feedstocks based on preliminary results. 10 g of prepared feedstock was loaded into the reactors with a total volume of 30.0 mL. The reactor setup was augmented with a high-pressure valve to regulate pressure, as well as for collection of the final gas product. As described, the reactor assembled before sealing and purging the headspace with nitrogen gas to displace atmospheric gases and to confer an initial pressure of 0.5 MPa. A tube furnace with electric resistance heating (Thermo Scientific Lindberg Blue M) was used to maintain the desired temperature for each particular reaction condition. The furnace was preheated, and then, the reactor was inserted for the reaction time to begin after heating for 3–4 min, accounting for when the reactor surface reached the desired temperature. The experiments were conducted in duplicate for each condition with each feedstock, and the results are presented as the average with standard errors.

When the complete reaction time was achieved, the reactor was removed from the furnace and cooled by saturation with room temperature water for 3 min to stop the reaction immediately. The gas valve was use to verify the pressure and, then, released for collection in a gas bag. A gas chromatograph (Shimadzu Gas Chromatograph, GC-17A) with a TCD detector was used to analyze the sample. The GC column was packed with silica gel, 18 ft. long, and presented an outer diameter of 1/8″, and the temperature of the injector, detector, and column were set to 160 °C, 150 °C, and 140 °C, respectively.

After reaction completion, three washes of 5 mL with dichloromethane (DCM, CH_2Cl_2) were used for solvent recovery of the oil product and residues from the reactor. Vacuum filter separation was performed on the recovered mixture of HTL products, and the liquid and solid phases were separated first. First, the solids were isolated and quantified using pre-weighted filter papers (Whatman No.4). Then, the aqueous fraction and biocrude oil with dichloromethane (DCM) solvent that passed through the filter were transferred to a separatory funnel. After complete phase separation, the biocrude oil and aqueous phase were recovered in separate vials and allowed to sit for evaporation of the recovery solvent. The biocrude oil and aqueous phase products were collected and quantified by weight before subsequent analysis.

2.4. Gas Chromatography Mass Spectroscopy (GC–MS)

Analysis of the hydrothermal liquefaction aqueous phase product was performed with a 2 μL sample that was injected into a GC–MS system composed of an Agilent 6890 gas chromatograph, an Agilent 5973 mass selective detector, and an Agilent 7683B autosampler set up in split mode (10:1). A 60 m ZB-5MS column with a 0.32 mm nominal diameter and 0.25 μm film thickness, using an injection temperature of 250 °C and Mass Selective Detector transfer line at 250 °C was used for gas chromatography. The oven temperature was initially set to 70 °C with a hold time of 2 min, then increased at 5 °C·min^{-1} until reaching 300 °C, and held constant for 5 min. The source temperature was 230 °C, electron ionization was set at 70 eV, and spectra were scanned from 30 to 800 *m/z*. Individual peaks were identified by matching fragmentation patterns against a NIST (NIST08) database, and then, analysis of the output was performed to identify and categorize compounds resulting from the various HTL reactions.

2.5. Inductively Coupled Plasma Optical Emission Spectrometry

Analysis of the aqueous and solid products was performed using Thermo Scientific iCAP 7600 Inductively Coupled Plasma Optical Emission Spectrometry (ICP-OES) Duo and associated Thermo Scientific Qtegra software, combined with a Sprint Valve. Calibration standards were prepared from a custom multiple element stock standard, SCP Science's Plasma CAL Custom Standard that includes certified concentrations of all 27 elements, and an additional two reference materials were used to check the calibration, Inorganic Ventures Multi Analyte Custom Grade Solutions (CCS-4, CCS-5, and CCS-6) and SCP Science's Matrix Reference Material EnviroMAT Ground water High (ES-H). The calibration is checked every 10–15 samples with a recalibration, recalculation, and reacquisition when the calibration check fails. Sample concentrations were reported as the average of three repeated measurements.

2.6. Nutrient analysis

Measurements for ammonia nitrogen, total nitrogen (TN), and chemical oxygen demand (COD) were performed on all hydrothermal liquefaction aqueous phase (HTL-AP) from the various feedstocks and reaction conditions. These samples were evaluated in accordance with American Public Health Association (APHA, 2012) standards using Hach methodologies: 8038, 10,072, and 8000, respectively. Each test was calibrated with standard solutions, and all measurements were performed in triplicate. The readings were performed using a Hach spectrophotometer (Model DR3900). The results are presented as average values with standard deviations.

3. Results and discussion

3.1. Effect of feedstock composition on product yield

A principal component analysis (PCA) was performed on the range of HTL reaction time and temperature for the different food wastes. PCA serves to identify data object relationships that are evaluated with eigenvalues that can be interpreted as the significance of the correlation (0–0.25: poor; 0.25–0.5: moderate; 0.5–0.75: strong). In this study, the eigenvalues among the three feedstock composition (Lipid, Protein, and Carbohydrate) and three HTL product streams (oil, aqueous, and solids) were correlated. Variables that present better correlation are more proximally located on the chart, being either positive or negative based on the axis, and the percentages of each axis correspond to percent variance of the total explained by the principal components. Fig. 1 presents the correlations among distributions of feedstocks and HTL product mass distribution. For example, the strongest correlation existed between the lipids and oil yield, as indicated by the proximity of the arrows and an eigenvalue of approximately 0.46. In contrast, a strong correlation was shown between the solid yield and the feedstock carbohydrate content. The carbohydrates group, encompassing bread, vegetables, and peels, were able to be correlated with an eigenvalue of 0.48; however, some of these points fell further away from the principal cluster of points located on the negative x axis between quadrants 2 and 3. The least significant correlation of the three couplings was between the protein rich feedstocks and aqueous product yields, resulting in an eigenvalue of 0.24. Most chicken and beef were correlated, as they were plotted in the same quadrant regardless of reaction time and temperature, however, there was a greater disparity in correlating these points directly to HTL aqueous product yield. This information corroborates previous PCA analysis performed in assessing feedstock composition influence on HTL product output (Watson et al., 2020), and the composition of these byproducts warrants their characterization and valorization.

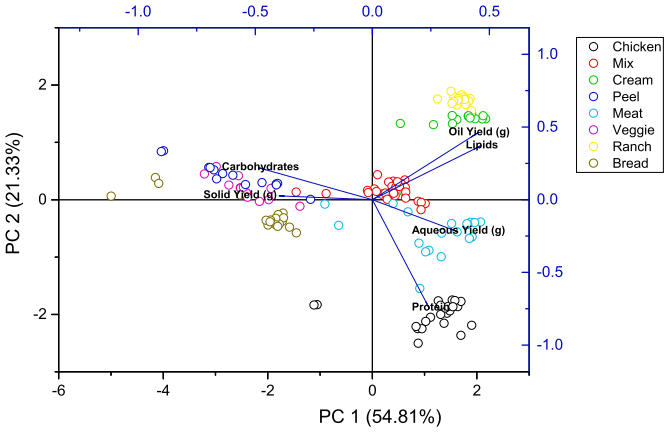

Fig. 1. Principal component analysis (PCA) correlating feedstock compositions to HTL products yield. The various colors represent the different feedstocks and the total HTL reaction conditions (280–360C; 10–60 min).

The corresponding oil yield values, as well as an updated model for predicting biocrude yield based on feedstock composition and HTL reaction severity, was also reported by Aierzhati et al. (2019). The optimized conditions for the lipid rich feedstocks were the highest oil yielding (70–80%), followed by protein (35–55%) and carbohydrates (10–40%). The literature has numerous reports of lipid rich feedstocks being favorable for oil production via HTL processes (Li et al., 2014; Yang et al., 2019), corroborating the highest yield of up to 80% in the present study. This result is very promising for HTL development and feedstock selection, as these are higher than many of the feedstocks typically used, such as: manure (25–45%), algae (12–64%), lignocellulosic residues (10–45%), among others (Dimitriadis and Bezergianni, 2017; Elliott et al., 2015). One reason these lipid-rich cream cheese and salad dressing residues can generate such oil yields in optimal HTL conditions is because the various monounsaturated fatty acids (MUFA), polyunsaturated fatty acids (PUFA), and fatty acids in general have low energy requirements for direct conversion to hydrocarbons (Hietala et al., 2017). This emphasizes using high lipid feedstocks for efficient conversion and increased oil recovery.

There is less available information on conditions that influence byproduct distribution and properties. Some inferences can be made from the present results to explain product generation with respect to the feedstock compositions. The solid phase is comprised mostly of metals and other inorganic material, resulting in high ash content (Cantero-Tubilla et al., 2018), while the aqueous yield is more dependent on nitrogen and water and solvent reactions. Accumulation of these elements and compounds in can be attributed to less severe reaction conditions (lower temperature and time), charring/carbonification/condensation reactions, and methods for separating the different productions from HTL reactions (Watson et al., 2020; Yang et al., 2016). Moreover, research on HTL reaction kinetics has shown favor for production of solid products from carbohydrate rich feedstocks (Obeid et al., 2019). Further modeling of byproduct specific reactions could describe possible outcomes, but the HTL conditions range of the present study promote data variability and limit achieving both higher eigenvalue and stronger correlations.

3.2. Reaction severity dependent nutrient distribution

Fig. 2 describes the total nitrogen (TN), ammoniacal nitrogen (NH_x), and chemical oxygen demand (COD) content of the aqueous phases produced across reaction temperatures. Among all the analyzed aqueous phases, the protein rich feedstocks, chicken and ground beef, resulted in the greatest concentrations of nitrogen and COD species. These nitrogen and COD values ranged from 5000–25,000 and 75,000–220,000 $mg{\cdot}L^{-1}$ (ppm), respectively, while the values ranged from 1000–8000 and 40,000–130,000 $mg{\cdot}L^{-1}$ for carbohydrates and 500–3000 and 30,000–720,000 $mg{\cdot}L^{-1}$ for lipids, respectively. The relative concentrations reflect protein, lipid, or carbohydrate feedstock concentrations, molecular breakdown, and repolymerization under HTL conditions, as well as migration upon product separation. For example, there was a greater range of nitrogen species in the protein rich feedstock aqueous phases, and thus, the simultaneous increase in COD species was the result of accumulated ammoniacal nitrogen, amino acids, or other nitrogen compounds. The protein group presented the greatest concentrations of nitrogen or COD and was followed in concentration by the carbohydrate and lipid feedstocks with the exception of peel.

As temperature was increased, there was a decreasing trend for total nitrogen, while there is an increase in ammoniacal nitrogen. This can be explained by the breakdown of proteins and peptide bonds, as well as other nitrogen containing compounds, under increased severity of HTL conditions, and it is likely that these water-soluble species migrate to the aqueous reaction solvent (Lu et al., 2018a; Obeid et al., 2019). This phenomenon typically results in between 30 and 70% ammoniacal

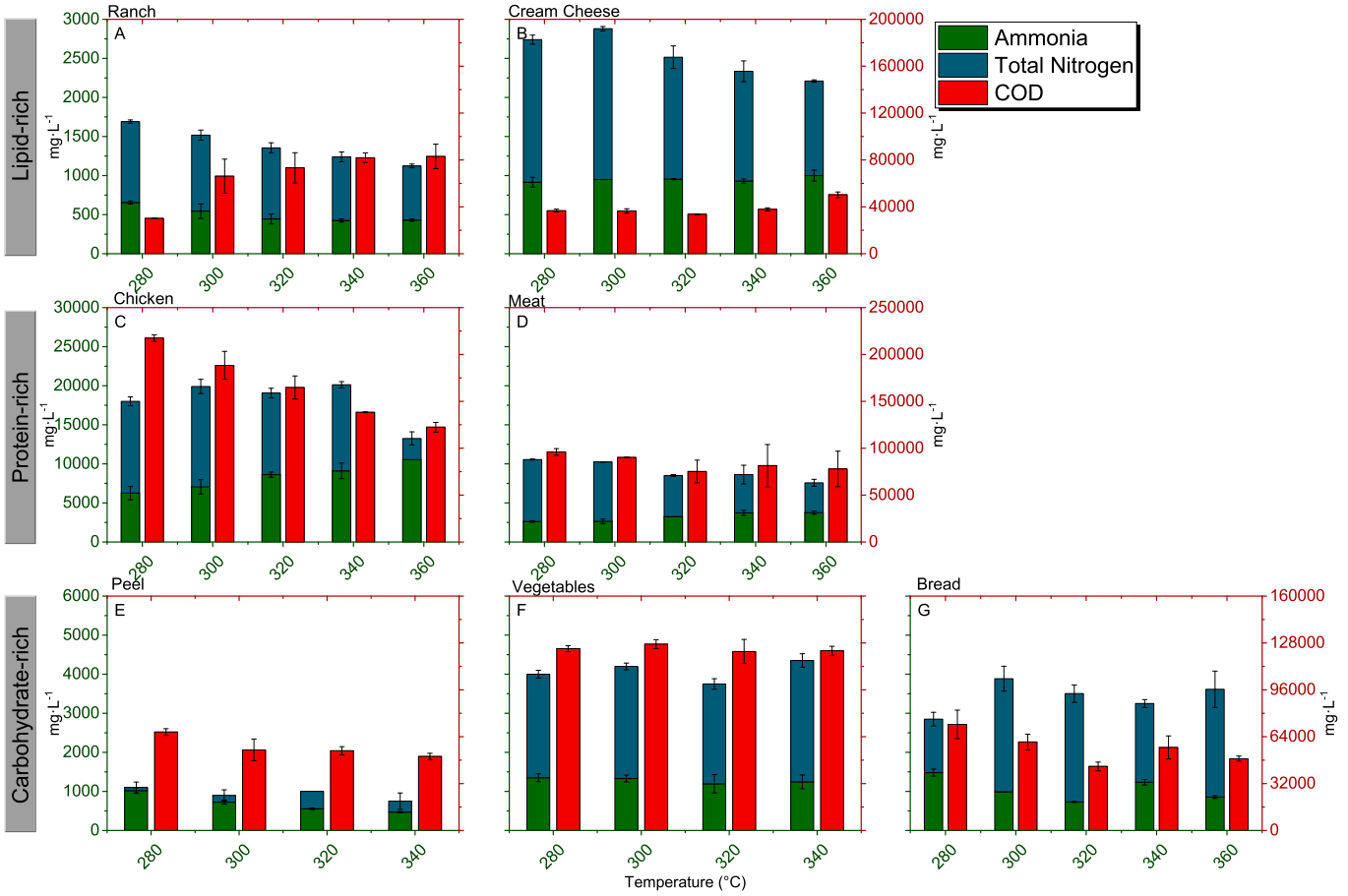

Fig. 2. Distribution of total nitrogen, ammoniacal nitrogen, and chemical oxygen demand across range of HTL reaction temperatures for the different feedstocks. Lipid-rich, Protein-rich, and Carbohydrate rich feedstocks are arranged in the top, middle, and bottom rows, respectively (Total Nitrogen = Blue and Ammoniacal Nitrogen = Green, both corresponding to the left y-axis, while COD = Red, corresponding to the right y-axis).

nitrogen depending on feedstock, reaction conditions, and different separation parameters (Watson et al., 2020). Accumulation of ammoniacal nitrogen potentiates its use in production agriculture systems as a readily available form of nitrogen to organisms. However, other aqueous phase nitrogen forms or components could require pretreatment to facilitate assimilation and incorporation into biological processes. The potency of these nitrogen species, as well as other requisite nutrients, is discussed in Section 3.5.

Fig. 3 describes the TN, NH_x, and COD content of the aqueous phases produced across the different reaction times. In comparison with temperature dependency, the decreasing trend for nitrogen content is less clear; however, there is again a clear trend of ammoniacal nitrogen accumulation as time increases. As the reaction severity increases, the ammoniacal species are liberated in the resultant HTL aqueous phase, likely because of protein breakdown into amino acids and nitrogen species. Some of these trends and molecule breakdown can be explained by expected pathways and hydrolytic depolymerization, described by Changi et al. (2015). The discrepancies between total nitrogen and ammonia can be attributed to a number of nitrogenous compounds, especially heterocyclic compounds. Many of these compounds with 1 nitrogen atom can be easily oxidized, partly releasing ammonia, nitrogen gas or other compounds (Chudoba and Dalešický, 1973). Noting this relationship between COD and the heterocyclic compounds, the COD value trends down for all feedstocks as time increases, except for ranch. These species could oxidize or migrate to other HTL product phases as the reaction supersedes the ideal time for each optimized feedstock temperature.

The peel feedstock stands out among the described trends. This feedstock is a particular exception as it is typically comprised of more carbohydrate or cellulosic material, which lowers biocrude production, often generates solid material (Zhu et al., 2017), and could lower nutrient availability and downstream recovery from HTL-AP. Therefore, it could be labeled among the worst of feedstocks for HTL processes and value recovery. On the other hand, the C:N ratio of the peel and bread HTL-AP is approximately 28 and 20, respectively, and is considerably higher than other feedstocks ranging from 2 to 10, validating its use in anaerobic digestion systems. The peel solid phase, in this light, also presents some favorable production qualities and composition, making its reuse advantageous, but applications are currently limited (López Barreiro et al., 2013). Thus, further study on pretreatment of such feedstocks is needed in order to balance nutrient availability and value recovery peel HTL products.

3.3. Hydrothermal liquefaction aqueous phase organics abundance and classification

Fig. 4 presents the Gas Chromatography-Mass Spectroscopy (GC–MS) results of the aqueous phase for the ideal HTL reaction conditions of each food waste feedstock, organized into composition groups for comparison. The compound groups assessed include: short chain acids, alcohols, amines, benzoic acid and derivatives, cyclic hydrocarbons, phenols, amides, heterocyclic nitrogen compounds, oxygen compounds, ketones and aldehydes, and a small fraction that fell outside of these classifications, such as carbon dioxide and methylene chloride. Some compounds identified in this study were accounted for as outputs of the specific GCMS methodology and NIST database

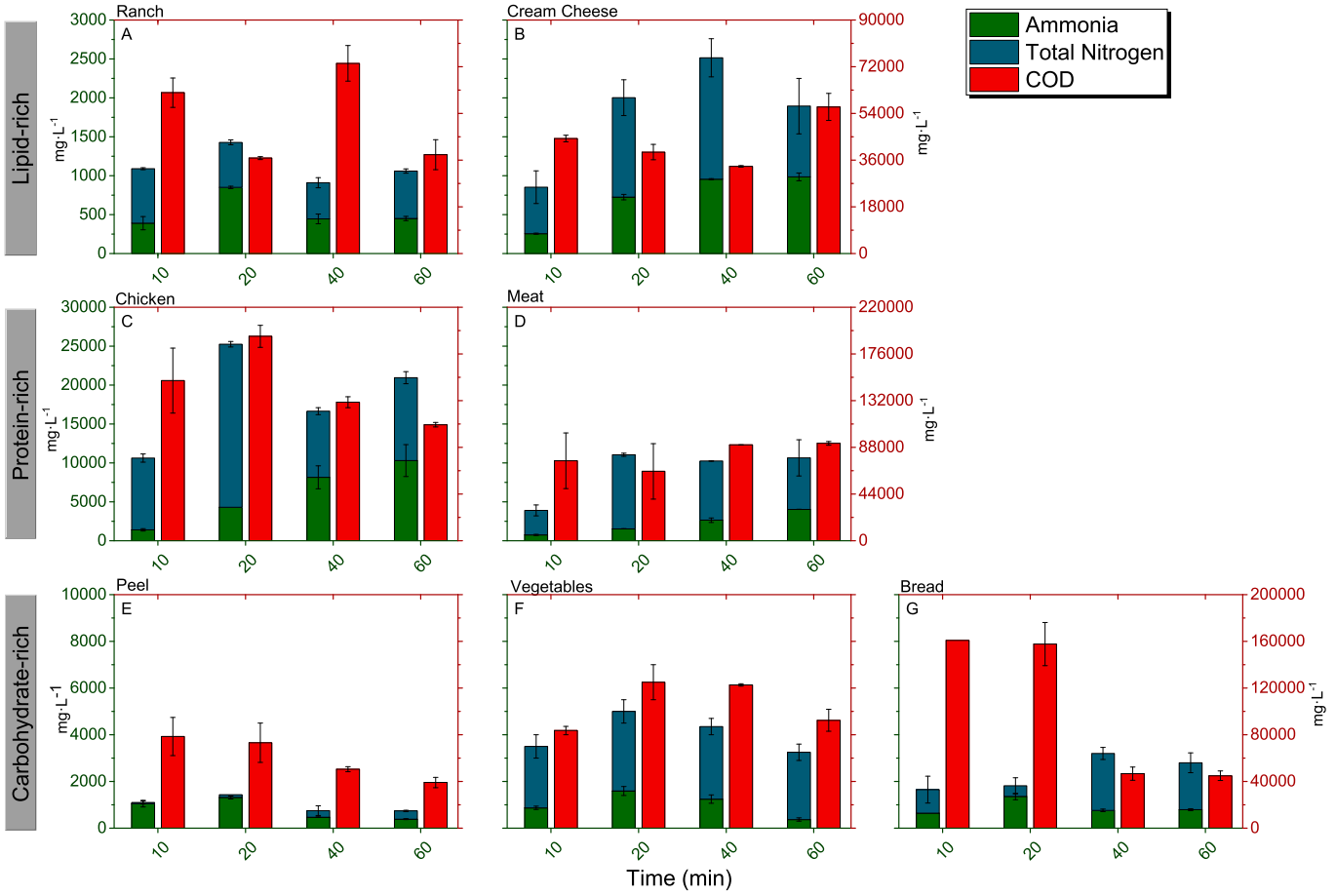

Fig. 3. Distribution of total nitrogen, ammoniacal nitrogen, and chemical oxygen demand across range of HTL reaction times for the different feedstocks. Lipid-rich, Protein-rich, and Carbohydrate rich feedstocks are arranged in the top, middle, and bottom rows, respectively (Total Nitrogen = Blue and Ammoniacal Nitrogen = Green, both corresponding to the left y-axis, while COD = Red, corresponding to the right y-axis).

identification and analysis. The radar plots show the cumulative relative abundance of peak areas of each of these categories identified from the GC–MS output in accordance with similar classifications for HTL-AP (Tommaso et al., 2015; Zheng et al., 2017). These authors discussed also potential benefits or drawbacks in its application and treatment with downstream biological processes while.

Short chain acids were observed as the most prevalent species among almost all of the food groups. These compounds can result from the breakdown of sugars or triglycerides, which are typically modelled HTL compounds. Hydrothermal reactions facilitates separation carbon and hydrogen chains of varying sizes and hydrogenation processes that generate predominantly biocrude oil products, in addition other aqueous phase constituents (Yu et al., 2011). The relative high abundance could suggest the favorable reformation or polymerization of short chain acid molecules. The resultant partitioning of these molecules and between different HTL products can be dependent on a number of factors, including feedstock qualities and reaction conditions (Vardon et al., 2011), extraction solvents (Watson et al., 2019), molecular interactions (Shakya et al., 2017), among others. The accumulation of these short chain acids, notably acetic acid, has demonstrated potential for HTL-AP recycling, both serving as a catalyst to derive greater biocrude yield in subsequent HTL reactions and as a substrate for microorganisms (Biller et al., 2016; Hu et al., 2017).

The heterocyclic nitrogen compounds ranged between 5 and 45% in the GC–MS compound compositions. The highest concentration was observed in the bread group, and this observation could be attributed to the abundance of carbohydrates, especially hydrolyzed into monosaccharides. These heterocyclic compounds are formed as a result of carbohydrate monomers and amino acids, known as the maillard reaction (Qiu et al., 2019; Sheng et al., 2018). Phenols are also a group of compounds reported to inhibit biological systems like algal and anaerobic digestion; however, these compounds were not identified in the GCMS outputs. While it might be expected in the highest concentrations for lignin-based feedstocks like the fruit peels or vegetables, less cellulosic groups in the group substrates could explain the absence of phenolic groups.

These hydrothermal liquefaction aqueous phase (HTL-AP) constituents have also been previously quantified and assessed for toxicity in mammalian cells (Pham et al., 2013b). Other researchers have similarly categorized them to determine inhibition in anaerobic digestion assays (Tommaso et al., 2015), and to specifically confer toxic affects to algae growth (Biller et al., 2012; Leng et al., 2018). While identification and analysis methods have been advanced to help in HTL-AP characterization and valorization, study of both these compounds benefits and their toxicity with microbial assays and nutrient availability are still limiting factors in their downstream processing, considering their specific inhibitory effects in cellular functions (Leng et al., 2018; Pham et al., 2013a).

3.4. Metals and nutrient element concentration

Fig. 5 presents the concentrations of various metals and elements in both the HTL aqueous (a) and solids phase (b) from the different food waste feedstocks for their respective optimized reaction conditions (highest biocrude oil yield). It should also be noted that the ideal conditions for HTL of the chicken feedstock did not yield a solid

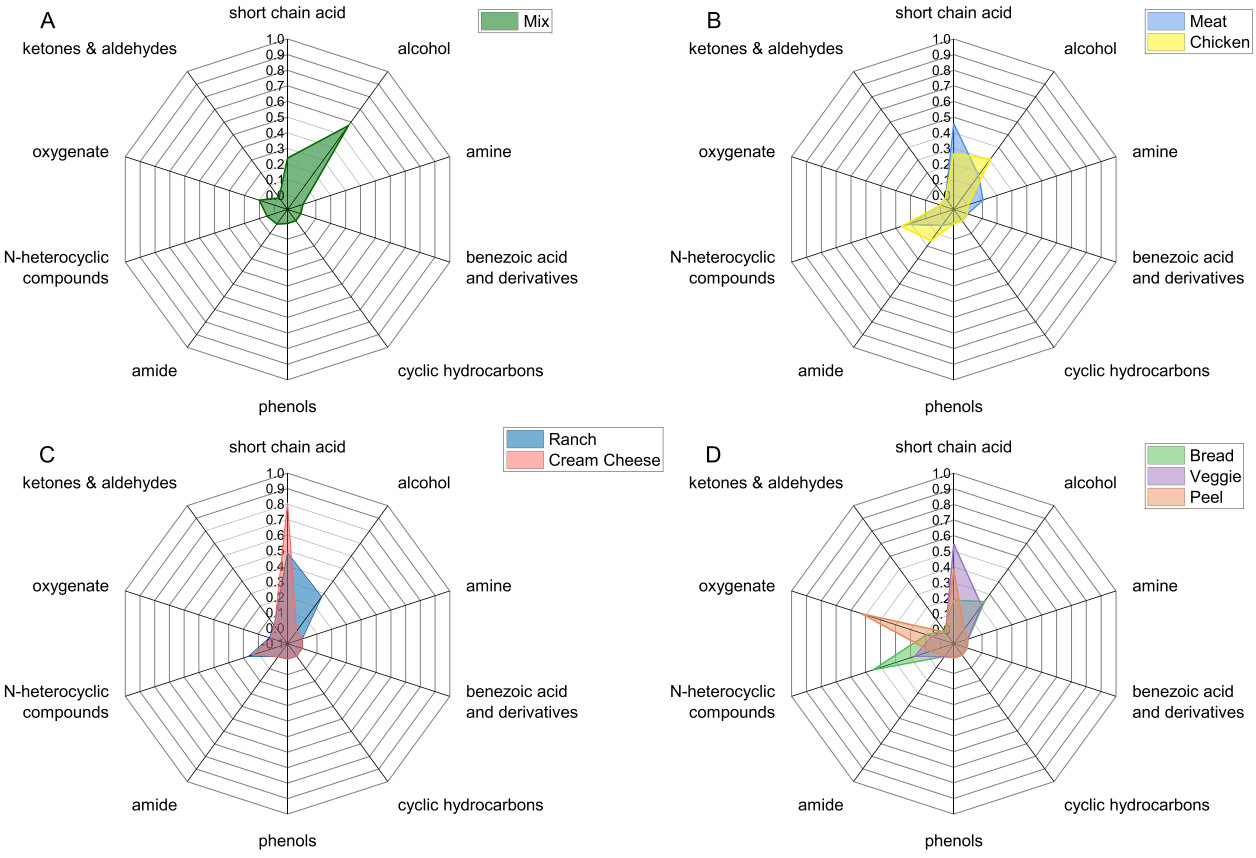

Fig. 4. Radar charts presenting the GC–MS compound classifications for the hydrothermal liquefaction aqueous phase (HTL-AP) of the optimized HTL reaction conditions for each of the different food waste feedstocks (A: Mix; B: Protein Group; C: Lipid Group; D: Carbohydrate Group).

product. The concentrations of these elements was as much as 16-fold greater in the solid material, as also previously reported (Zhu et al., 2017). The total accumulation of metals is a key appeal for HTL solid reuse, which result from insoluble metal complexes in different solvents, such as water and acetone (Lu et al., 2018b). For example, several platinum group metals, such as copper, iron, and aluminum, were in higher relative abundance in comparison to other societal wastes previously identified for value recovery (Raikova et al., 2019), and this justifies their recovery from HTL solids through different mechanisms.

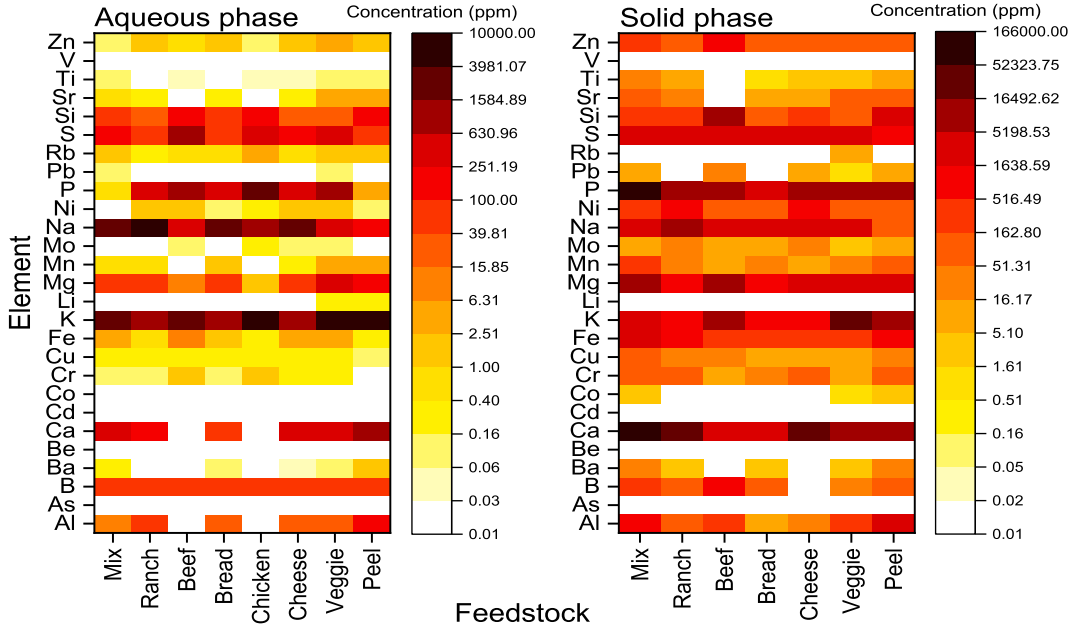

Fig. 5. Heat map quantifying various metals and elements measured in the (a) aqueous and (b) solids phase of the optimized HTL reaction conditions for each of the different food waste feedstocks.

The most concentrated elements in the solids include: calcium, magnesium, and phosphorus. This observation can be attributed to food waste materials like eggshell particulate matter observed in the campus dining hall mix. Notably, phosphorus potentiates its reuse in production agricultural systems as it is requisite for life systems and can be a limited resource. On the other hand, some heavy metals were also identified, including lead and chromium, while arsenic and cadmium were below the detection levels. These metals are of concern in food systems, posing risk in reuse for lettuce cultivation for example (Jesse and Davidson, 2019). Some elements stand out as particular to the solid phase, cobalt in particular. This is of significance for the HTL-AP reuse in algae cultivation, notably being limited in comparison to algal media concentrations (Jena et al., 2011). Cobalt serves as key component in cobalamin, vitamin B12, which is a cofactor for enzymes that participate in rearrangement-reduction reactions or methyl transfer reactions, being requisite in bacterial, algal, and mammalian systems. The absence of cobalt, thus, suggests it must be recovered from the solid phase or be supplemented in HTL-AP to be made available for biological processes. Generally, such metals serve in several capacities to facilitate cellular functions for maintaining homeostasis, and further research on HTL byproducts must also evaluate metal speciation for making these elements available to cells in different environments (Martinez-Finley et al., 2012).

Notably, calcium, magnesium, phosphorus, potassium, sodium, sulfur, and silicon are among the most abundant elements in the HTL-AP, as also previously reported (Jiang and Savage, 2018). Their abundance, can be explained by relevance in agricultural or food production and other biological processes (Jena et al., 2011). Thus, these food waste HTL-AP processes and characterization can serve as a benchmark for use in downstream bioremediation processes, as previously suggested (Raikova et al., 2019). Among applications for HTL-AP, there are several elements with potential use as fertilizer and food production substrates, but further investigation is needed to investigate how these elements accumulate and are sequestered by biological systems, especially metals, based on their availability (Jesse et al., 2019).

3.5. Biological nutrient availability

The heat map approach can also be used in developing novel application or pretreatment hypothesis for the aforementioned downstream biological processes. Fig. 6 presents a comparison of nutrients in the HTL-AP and between a two cultivation media recipes: one for algae cultivation (Stanier et al., 1971) and the other for anaerobic digestion (Angelidaki et al., 2009). The scale percentage values reflect the molar concentration of the raw elements within the different HTL-AP as compared to their prescribed concentration in ideal nutrient mixtures. For example, cobalt was not observed in the different HTL-AP, and thus, there is 0% availability when compared to the nutrient assays for algae and AD. On the other hand, 1000% percent means the molar concentration in the HTL-AP is 10 times in excess of the recommended value for the respective media. Thus, elements like potassium and boron are in significant abundance, and ammonium, referenced from the nutrient data, and is also in excess for media requirements. Thus, reuse of the HTL-AP is very promising for its rich concentration of nutrients, while some components would require significant dilution when presenting inhibitory effects, as previously reported for algae (Biller et al., 2012; Jena et al., 2011), which is a novel comparison.

Appropriating these nutrients for reuse in biological systems is often coupled with determining their toxicity in single cells strains (Biller et al., 2012; Pham et al., 2013b), algal polycultures (Godwin et al., 2017), or robust bacterial cultures like AD (Zhou et al., 2015). However, the present study offers a broad assessment of the nutrient availabilities between differentially produced HTL-AP and the nutrient requirements for two potential biological systems. Again, there was minimal detection of heavy metals, making their use in food production seemingly feasible. Among these feedstocks, the mix food waste and peel groups stand out as deficient in phosphorus. Similarly, the protein feedstocks lacked some essential metals, such as manganese and magnesium for both cell types, and aluminum for anaerobic digestion in particular. Cobalt was lacking across all feedstocks and would be a limiting factor in the use of HTL-AP for downstream biological processes without augmentation.

The numerous inhibitory compounds, such as heterocyclic nitrogen and phenolic compounds, and their effects on cells are a focal consideration (Pham et al., 2013b). Dilution has been widely used for pretreating HTL-AP in such systems, but new approaches for reducing these compounds, such as thorough feedstock and reaction conditions evaluation would significantly contribution to reuse applications, as well as integration of HTL systems overall. Limited review of HTL-AP inhibition in cells mechanisms (Li et al., 2020) warrants further study determine factors, such as cause or distribution of elemental species, specific availability or effects on cells, and pretreatments that could improve availability in downstream biological applications.

4. Prospects and technological applications

Given the variability of food waste feedstock and resultant HTL byproduct composition, future research should target substrate mixtures or pretreatment that will improve either biocrude production or alternatively create ideal conditions for byproduct reuse. Among abundant sources for such agricultural and food processing waste for HTL, some large producing locations can be highlighted: production agriculture farms, processing plants, grocery stores, waste disposal sites, etc. These locations could be ideal for collection of these feedstocks for HTL processing and biocrude or byproduct generation, based on their elemental and molecular compositions (Pavlovič et al., 2013). For example, dairy processing plants, dining hall grease pits, and lipid collection tanks for anaerobic digesters should all be considered potential collection sites for high oil yielding feedstocks, as these could improve the application and viability of HTL operations. However, the quantity and composition of such HTL products could also contain significant portions of fatty acid and, thus, increase biocrude oxygen content (Vardon et al., 2011; Watson et al., 2020), which affects their downstream processing and intended use. Certain agricultural residues, animal manure and carcasses for example, may present increased protein and carbohydrate content and, thus, be processed with HTL to amplify nutrient concentration and recycling (Zhou et al., 2013) or metals for alternative market applications, respectively. Overall, HTL applications can become more economically and environmentally viable to improve conditions for and implementation through these diversification strategies.

5. Conclusions

The present results analyzed the elemental and molecular composition of HTL food waste solids and HTL-AP, based on feedstock composition and reaction conditions to identify opportunities and bottlenecks in resource recovery. HTL reaction conditions severity demonstrated breakdown and reformation of different molecule classes, for potentiating downstream systems application and limiting factors. The high availability of diverse metals present opportunity for use in biological media, notably through metal recovery and nutrients for algae cultivation or anaerobic digestion. These benchmarks for nutrient concentrations and availability assess differences between HTL products based on optimized operating conditions for food waste.

Declaration of competing interest

We wish to confirm that there are no known conflicts of interest associated with this publication and there has been no significant financial support for this work that could have influenced its outcome.

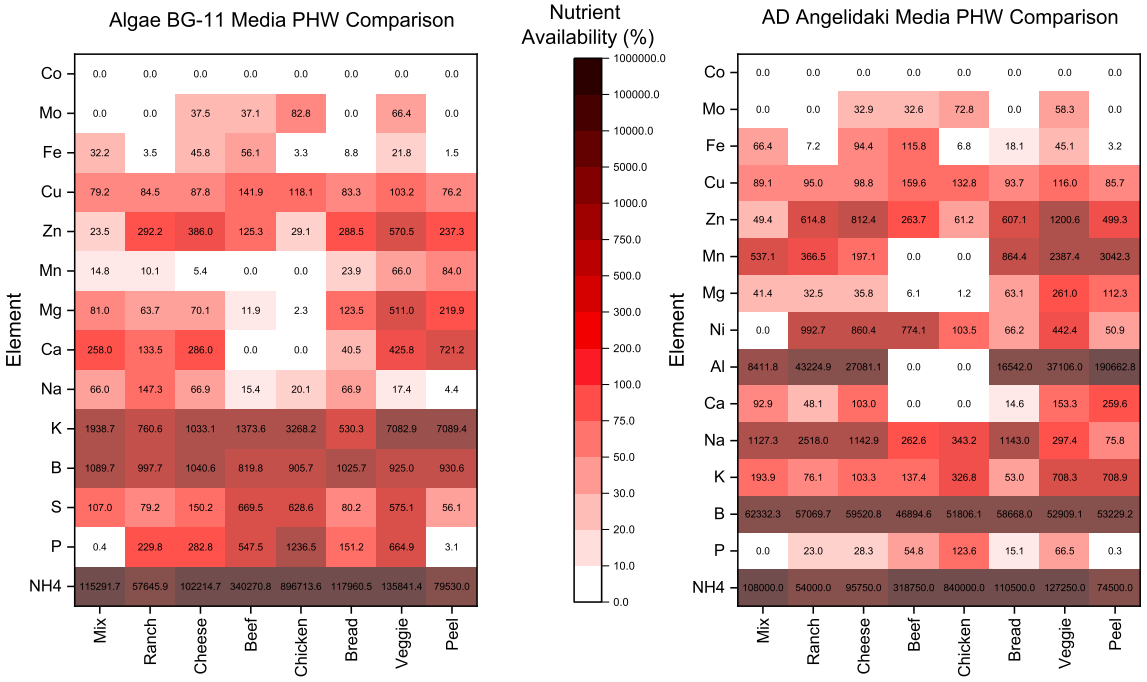

Fig. 6. Heat map prospecting nutrient availability by comparing molarity based element concentrations of (a) algae and (b) anaerobic digestion nutrient mixtures to measured values in HTL-AP from optimized reaction conditions for each of the different food waste feedstocks.

Acknowledgements

The authors would like to acknowledge financial support from the University of Illinois at Urbana Champaign Student Sustainable Committee (SSC), and the National Science Foundation (NSF CBET 17-44775).

References

Aierzhati, A., Stablein, M.J., Wu, N.E., Kuo, C.T., Si, B., Kang, X., Zhang, Y., 2019. Experimental and model enhancement of food waste hydrothermal liquefaction with combined effects of biochemical composition and reaction conditions. Bioresour. Technol. 284, 139–147. https://doi.org/10.1016/j.biortech.2019.03.076.

American Public Health Association (APHA), A.W.W.A. (AWWA) and W.E.F. (WEF), 2012. Standard Methods for the Examination of Water and Wastewater, 22nd ed. Washington DC.

Angelidaki, I., Alves, M., Bolzonella, D., Borzacconi, L., Campos, J.L., Guwy, A.J., Kalyuzhnyi, S., Jenicek, P., Van Lier, J.B., 2009. Defining the biomethane potential (BMP) of solid organic wastes and energy crops: a proposed protocol for batch assays. Water Sci. Technol. 59, 927–934. https://doi.org/10.2166/wst.2009.040.

Biller, P., Ross, A.B., Skill, S.C., Lea-Langton, A., Balasundaram, B., Hall, C., Riley, R., Llewellyn, C.A., 2012. Nutrient recycling of aqueous phase for microalgae cultivation from the hydrothermal liquefaction process. Algal Res. 1, 70–76. https://doi.org/10.1016/J.ALGAL.2012.02.002.

Biller, P., Madsen, R.B., Klemmer, M., Becker, J., Iversen, B.B., Glasius, M., 2016. Effect of hydrothermal liquefaction aqueous phase recycling on bio-crude yields and composition. Bioresour. Technol. 220, 190–199. https://doi.org/10.1016/J.BIORTECH.2016.08.053.

Cantero-Tubilla, B., Cantero, D.A., Martinez, C.M., Tester, J.W., Walker, L.P., Posmanik, R., 2018. Characterization of the solid products from hydrothermal liquefaction of waste feedstocks from food and agricultural industries. J. Supercrit. Fluids 133, 665–673. https://doi.org/10.1016/J.SUPFLU.2017.07.009.

Cao, L., Zhang, C., Chen, H., Tsang, D.C.W., Luo, G., Zhang, S., Chen, J., 2017. Hydrothermal liquefaction of agricultural and forestry wastes: state-of-the-art review and future prospects. Bioresour. Technol. 245, 1184–1193. https://doi.org/10.1016/J.BIORTECH.2017.08.196.

Changi, M., S., L., Faeth, J., Mo, N., E. Savage, P., 2015. Hydrothermal reactions of biomolecules relevant for microalgae liquefaction. Ind. Eng. Chem. Res. 54, 11733–11758. https://doi.org/10.1021/acs.iecr.5b02771.

Chen, W.T., Zhang, Y., Lee, T.H., Wu, Z., Si, B., Lee, C.F.F., Lin, A., Sharma, B.K., 2018. Renewable diesel blendstocks produced by hydrothermal liquefaction of wet biowaste. Nat. Sustain. 1, 702–710. https://doi.org/10.1038/s41893-018-0172-3.

Chudoba, J., Dalešický, J., 1973. Chemical oxygen demand of some nitrogenous heterocyclic compounds. Water Res. 7, 663–668. https://doi.org/10.1016/0043-1354(73)90084-5.

Danthurebandara, M., Passel, S., Nelen, D., Tielemans, Y., Van Acker, K., 2013. Environmental and Socio-economic Impacts of Landfills.

Dimitriadis, A., Bezergianni, S., 2017. Hydrothermal liquefaction of various biomass and waste feedstocks for biocrude production: a state of the art review. Renew. Sust. Energ. Rev. https://doi.org/10.1016/j.rser.2016.09.120.

Elliott, D.C., Biller, P., Ross, A.B., Schmidt, A.J., Jones, S.B., 2015. Hydrothermal liquefaction of biomass: developments from batch to continuous process. Bioresour. Technol. 178, 147–156. https://doi.org/10.1016/J.BIORTECH.2014.09.132.

Environmental Protection Agency, 2019. Advancing Sustainable Materials Management: 2017 Fact Sheet (pp. 1-12, Rep. No. 530-F-19-007). Washington DC. https://www.epa.gov/sites/production/files/2019-11/documents/2017_facts_and_figures_fact_sheet_final.pdf.

Godwin, C.M., Hietala, D.C., Lashaway, A.R., Narwani, A., Savage, P.E., Cardinale, B.J., 2017. Algal polycultures enhance coproduct recycling from hydrothermal liquefaction. Bioresour. Technol. 224, 630–638. https://doi.org/10.1016/J.BIORTECH.2016.11.105.

Gollakota, A.R.K., Kishore, N., Gu, S., 2018. A review on hydrothermal liquefaction of biomass. Renew. Sust. Energ. Rev. 81, 1378–1392. https://doi.org/10.1016/J.RSER.2017.05.178.

Hietala, D.C., Koss, C.K., Narwani, A., Lashaway, A.R., Godwin, C.M., Cardinale, B.J., Savage, P.E., 2017. Influence of biodiversity, biochemical composition, and species identity on the quality of biomass and biocrude oil produced via hydrothermal liquefaction. Algal Res. 26, 203–214. https://doi.org/10.1016/J.ALGAL.2017.07.020.

Hu, Y., Feng, S., Yuan, Z., Xu, C. (Charles), Bassi, A., 2017. Investigation of aqueous phase recycling for improving bio-crude oil yield in hydrothermal liquefaction of algae. Bioresour. Technol. 239, 151–159. https://doi.org/10.1016/J.BIORTECH.2017.05.033.

Jena, U., Vaidyanathan, N., Chinnasamy, S., Das, K.C., 2011. Evaluation of microalgae cultivation using recovered aqueous co-product from thermochemical liquefaction of algal biomass. Bioresour. Technol. 102, 3380–3387. https://doi.org/10.1016/J.BIORTECH.2010.09.111.

Jesse, S.D., Davidson, P.C., 2019. Treatment of post-hydrothermal liquefaction wastewater (PHWW) for heavy metals, nutrients, and indicator pathogens. Water 11, 854. https://doi.org/10.3390/w11040854.

Jesse, S.D., Zhang, Y., Margenot, A.J., Davidson, P.C., 2019. Hydroponic lettuce production using treated post-hydrothermal liquefaction wastewater (PHW). Sustainability 11, 3605. https://doi.org/10.3390/su11133605.

Jiang, J., Savage, P.E., 2018. Metals and other elements in biocrude from fast and isothermal hydrothermal liquefaction of microalgae. Energy Fuel 32, 4118–4126. https://doi.org/10.1021/acs.energyfuels.7b03144.

Leng, L., Li, J., Wen, Z., Zhou, W., 2018. Use of microalgae to recycle nutrients in aqueous phase derived from hydrothermal liquefaction process. Bioresour. Technol. 256, 529–542. https://doi.org/10.1016/J.BIORTECH.2018.01.121.

Li, H., Liu, Z., Zhang, Y., Li, B., Lu, H., Duan, N., Liu, M., Zhu, Z., Si, B., 2014. Conversion efficiency and oil quality of low-lipid high-protein and high-lipid low-protein microalgae via hydrothermal liquefaction. Bioresour. Technol. 154, 322–329. https://doi.org/10.1016/J.BIORTECH.2013.12.074.

Li, H., Watson, J., Zhang, Y., Lu, H., Liu, Z., 2020. Environment-enhancing process for algal wastewater treatment, heavy metal control and hydrothermal biofuel production: a critical review. Bioresour. Technol. 298, 122421. https://doi.org/10.1016/J.

BIORTECH.2019.122421.
Liu, H.M., Li, H.Y., Li, M.F., 2017. Cornstalk liquefaction in sub- and super-critical ethanol: characterization of solid residue and the liquefaction mechanism. J. Energy Inst. 90, 734–742. https://doi.org/10.1016/j.joei.2016.07.004.
López Barreiro, D., Ronsse, F., Brilman, W., 2013. Hydrothermal liquefaction (HTL) of microalgae for biofuel production: state of the art review and future prospects. Biomass Bioenergy 53, 113–127. https://doi.org/10.1016/J.BIOMBIOE.2012.12.029.
Lu, J., Li, H., Zhang, Y., Liu, Z., 2018a. Nitrogen migration and transformation during hydrothermal liquefaction of livestock manures. ACS Sustain. Chem. Eng. 6, 13570–13578. https://doi.org/10.1021/acssuschemeng.8b03810.
Lu, J., Watson, J., Zeng, J., Li, H., Zhu, Z., Wang, M., Zhang, Y., Liu, Z., 2018b. Biocrude production and heavy metal migration during hydrothermal liquefaction of swine manure. Process. Saf. Environ. Prot. 115, 108–115. https://doi.org/10.1016/J.PSEP.2017.11.001.
Maddi, B., Panisko, E., Wietsma, T., Lemmon, T., Swita, M., Albrecht, K., Howe, D., 2017. Quantitative characterization of aqueous byproducts from hydrothermal liquefaction of municipal wastes, food industry wastes, and biomass grown on waste. ACS Sustain. Chem. Eng. 5, 2205–2214. https://doi.org/10.1021/acssuschemeng.6b02367.
Martinez-Finley, E.J., Chakraborty, S., Fretham, S.J.B., Aschner, M., 2012. Cellular transport and homeostasis of essential and nonessential metals. In: Metallomics. Royal Society of Chemistry, pp. 593–605. https://doi.org/10.1039/c2mt00185c.
Obeid, R., Lewis, D., Smith, N., van Eyk, P., 2019. The elucidation of reaction kinetics for hydrothermal liquefaction of model macromolecules. Chem. Eng. J. 370, 637–645. https://doi.org/10.1016/J.CEJ.2019.03.240.
Pavlovič, I., Knez, Ž., Škerget, M., 2013. Hydrothermal reactions of agricultural and food processing wastes in sub- and supercritical water: a review of fundamentals, mechanisms, and state of research. J. Agric. Food Chem. 61, 8003–8025. https://doi.org/10.1021/jf401008a.
Pham, M., Schideman, L., Scott, J., Rajagopalan, N., Plewa, M.J., 2013a. Chemical and biological characterization of wastewater generated from hydrothermal liquefaction of Spirulina. Environ. Sci. Technol. 47, 2131–2138. https://doi.org/10.1021/es304532c.
Pham, M., Schideman, L., Sharma, B.K., Zhang, Y., Chen, W.-T., 2013b. Effects of hydrothermal liquefaction on the fate of bioactive contaminants in manure and algal feedstocks. Bioresour. Technol. 149, 126–135. https://doi.org/10.1016/J.BIORTECH.2013.08.131.
Qiu, Y., Aierzhati, A., Cheng, J., Guo, H., Yang, W., Zhang, Y., 2019. Biocrude oil production through the maillard reaction between leucine and glucose during hydrothermal liquefaction. Energy Fuel 33, 8758–8765. https://doi.org/10.1021/acs.energyfuels.9b01875.
Raikova, S., Piccini, M., Surman, M.K., Allen, M.J., Chuck, C.J., 2019. Making light work of heavy metal contamination: the potential for coupling bioremediation with bioenergy production. J. Chem. Technol. Biotechnol. 94, 3064–3072. https://doi.org/10.1002/jctb.6133.
Shakya, R., Adhikari, S., Mahadevan, R., Shanmugam, S.R., Nam, H., Hassan, E.B., Dempster, T.A., 2017. Influence of biochemical composition during hydrothermal liquefaction of algae on product yields and fuel properties. Bioresour. Technol. 243, 1112–1120. https://doi.org/10.1016/J.BIORTECH.2017.07.046.
Sheng, L., Wang, X., Yang, X., 2018. Prediction model of biocrude yield and nitrogen heterocyclic compounds analysis by hydrothermal liquefaction of microalgae with model compounds. Bioresour. Technol. 247, 14–20. https://doi.org/10.1016/J.BIORTECH.2017.08.011.
Skaggs, R.L., Coleman, A.M., Seiple, T.E., Milbrandt, A.R., 2018. Waste-to-energy biofuel production potential for selected feedstocks in the conterminous United States. Renew. Sust. Energ. Rev. 82, 2640–2651. https://doi.org/10.1016/J.RSER.2017.09.107.
Stanier, R.Y., Kunisawa, R., Mandel, M., Cohen-Bazire, G., 1971. Purification and properties of unicellular blue-green algae (order Chroococcales). Bacteriol. Rev. 35, 171–205. https://doi.org/10.1128/mmbr.35.2.171-205.1971.
Tommaso, G., Chen, W.-T., Li, P., Schideman, L., Zhang, Y., 2015. Chemical characterization and anaerobic biodegradability of hydrothermal liquefaction aqueous products from mixed-culture wastewater algae. Bioresour. Technol. 178, 139–146. https://doi.org/10.1016/J.BIORTECH.2014.10.011.
Vardon, D.R., Sharma, B.K., Scott, J., Yu, G., Wang, Z., Schideman, L., Zhang, Y., Strathmann, T.J., 2011. Chemical properties of biocrude oil from the hydrothermal liquefaction of Spirulina algae, swine manure, and digested anaerobic sludge. Bioresour. Technol. 102, 8295–8303. https://doi.org/10.1016/J.BIORTECH.2011.06.041.
Wang, B., Huang, Y., Zhang, J., 2014. Hydrothermal liquefaction of lignite, wheat straw and plastic waste in sub-critical water for oil: product distribution. J. Anal. Appl. Pyrolysis 110, 382–389. https://doi.org/10.1016/J.JAAP.2014.10.004.
Watson, J., Lu, J., de Souza, R., Si, B., Zhang, Y., Liu, Z., 2019. Effects of the extraction solvents in hydrothermal liquefaction processes: Biocrude oil quality and energy conversion efficiency. Energy 167, 189–197. https://doi.org/10.1016/J.ENERGY.2018.11.003.
Watson, J., Wang, T., Si, B., Chen, W.-T., Aierzhati, A., Zhang, Y., 2020. Valorization of hydrothermal liquefaction aqueous phase: pathways towards commercial viability. Prog. Energy Combust. Sci. 77, 100819. https://doi.org/10.1016/J.PECS.2019.100819.
Yang, T., Wang, W., Kai, X., Li, B., Sun, Y., Li, R., 2016. Studies of distribution characteristics of inorganic elements during the liquefaction process of cornstalk. Energy Fuel 30, 4009–4016. https://doi.org/10.1021/acs.energyfuels.6b00096.
Yang, J., He, Q. (Sophia), Corscadden, K., Niu, H., Lin, J., Astatkie, T., 2019. Advanced models for the prediction of product yield in hydrothermal liquefaction via a mixture design of biomass model components coupled with process variables. Appl. Energy 233–234, 906–915. https://doi.org/10.1016/J.APENERGY.2018.10.035.
Yu, G., Zhang, Y., Schideman, L., Funk, T., Wang, Z., 2011. Distributions of carbon and nitrogen in the products from hydrothermal liquefaction of low-lipid microalgae. Energy Environ. Sci. 4, 4587. https://doi.org/10.1039/c1ee01541a.
Zheng, M., Schideman, L.C., Tommaso, G., Chen, W.-T., Zhou, Y., Nair, K., Qian, W., Zhang, Y., Wang, K., 2017. Anaerobic digestion of wastewater generated from the hydrothermal liquefaction of Spirulina: toxicity assessment and minimization. Energy Convers. Manag. 141, 420–428. https://doi.org/10.1016/J.ENCONMAN.2016.10.034.
Zhou, Y., Schideman, L., Yu, G., Zhang, Y., 2013. A synergistic combination of algal wastewater treatment and hydrothermal biofuel production maximized by nutrient and carbon recycling. Energy Environ. Sci. 6, 3765–3779. https://doi.org/10.1039/c3ee24241b.
Zhou, Y., Schideman, L., Zheng, M., Martin-Ryals, A., Li, P., Tommaso, G., Zhang, Y., 2015. Anaerobic digestion of post-hydrothermal liquefaction wastewater for improved energy efficiency of hydrothermal bioenergy processes. Water Sci. Technol. 72, 2139–2147. https://doi.org/10.2166/wst.2015.435.
Zhu, Z., Si, B., Lu, J., Watson, J., Zhang, Y., Liu, Z., 2017. Elemental migration and characterization of products during hydrothermal liquefaction of cornstalk. Bioresour. Technol. 243, 9–16. https://doi.org/10.1016/J.BIORTECH.2017.06.085.